

In Vitro Metabolic Stability and in Vivo Biodistribution of 3-Methyl-4-furoxancarbaldehyde Using PET Imaging in Rats

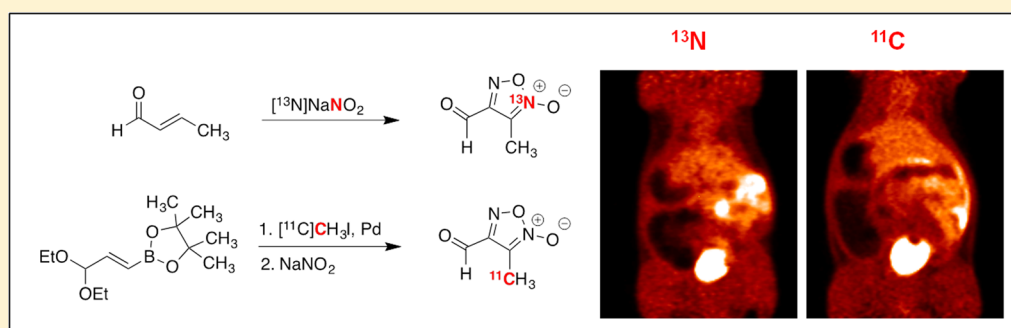
Adam B. Pippin,^{*,†,‡} Zaira Hidayah Mohd Arshad,[‡] Ronald J. Voll,[†] Jonathon A. Nye,[†] Sussan Ghassabian,[‡] Craig M. Williams,[§] Alessandra Mancini,[†] Dennis C. Liotta,^{‡,||} Maree T. Smith,^{‡,†} and Mark M. Goodman^{‡,†}

[†]Department of Radiology and Imaging Sciences, Emory University Center for Systems Imaging, Wesley Woods Health Center, 1841 Clifton Road, NE, Atlanta, Georgia 30329, United States

[‡]Centre for Integrated Preclinical Drug Development and [§]School of Chemistry and Molecular Biosciences, The University of Queensland, St Lucia Campus, Brisbane, Queensland 4072, Australia

^{||}Department of Chemistry, Emory University, 1521 Dickey Drive, Atlanta, Georgia 30322, United States

Supporting Information



ABSTRACT: Painful diabetic neuropathy (PDN) is a type of peripheral neuropathic pain that is currently difficult to treat using clinically available analgesics. Recent work suggests a progressive depletion of nitric oxide (NO) in nerve cells may be responsible for the pathobiology of PDN. The nitric oxide donor, 3-methyl-4-furoxancarbaldehyde (PRG150), has been shown to produce dose-dependent analgesia in a rat model of PDN. To gain insight into the mechanism of analgesia, methods to radiolabel PRG150 were developed to assess the *in vivo* biodistribution in rats. The furoxan ring was labeled with ¹³N to follow any nitric oxide release and the 3-methyl substituent was labeled with ¹¹C to track the metabolite using PET imaging. The *in vitro* metabolic stability of PRG150 was assessed in rat liver microsomes and compared to *in vivo* metabolism of the synthesized radiotracers. PET images revealed a higher uptake of ¹³N over ¹¹C radioactivity in the spinal cord. The differences in radioactive uptake could indicate that a NO release in the spinal cord and other components of the somatosensory nervous system may be responsible for the analgesic effects of PRG150 seen in the rat model of PDN.

KEYWORDS: Furoxan, nitric oxide (NO), 3-methyl-4-furoxancarbaldehyde (PRG150), positron emission tomography, biodistribution, metabolic stability

Nitric oxide (NO) is a well-known *in vivo* signaling molecule involved in many physiological and pathological processes.^{1,2} Biological synthesis occurs endogenously from L-arginine, oxygen, and NADPH by various nitric oxide synthase enzymes.¹ The gaseous nature of NO facilitates its free diffusion across cellular membranes, making it ideal for paracrine and autocrine signaling.² However, due to its existence as a gaseous free radical, NO is highly reactive and its *in vivo* action is restricted to limited areas. The extravascular half-life of NO is estimated at 0.09 to 2 s depending upon the O₂ concentration and the distance between blood vessels.³ Apart from activating the soluble guanylate cyclase and cyclic guanosine monophosphate (sGC/cGMP) signaling pathways, NO also regulates protein function by two chemical reactions: tyrosine nitration⁴ and S-nitrosation, also known as S-nitrosylation.⁵ These protein

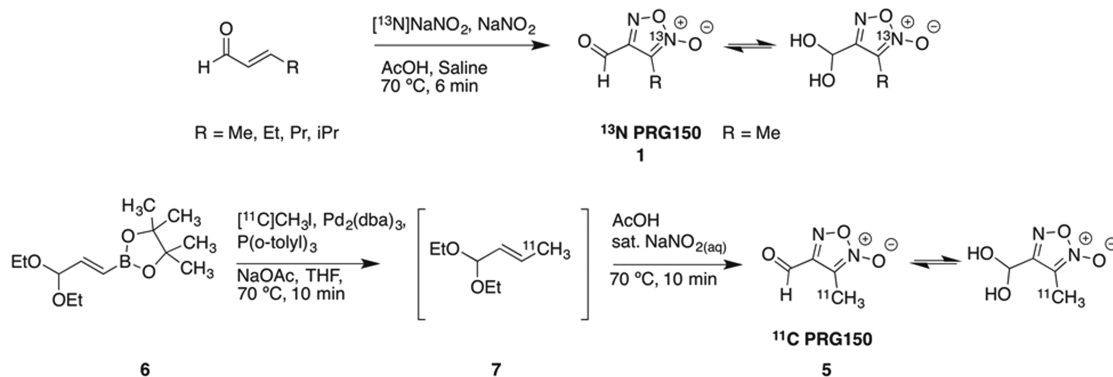
modifications play key roles in maintaining homeostasis in the cardiovascular system,⁶ learning and memory formation in the central nervous system,¹ modulation of skeletal muscle contractions,⁷ pain and nociception,⁸ and also play important roles in tumor biology and in inflammation.^{9,10}

Over the past decade, there has been significant research on the development of NO prodrugs to overcome the instability and inconvenient handling of aqueous NO solutions.² In particular, furoxans, a class of 5-membered heterocycles, have received significant attention as NO donors due to their wide range of

Received: October 20, 2015

Accepted: March 30, 2016

Table 1. Radiosynthesis of 3-Alkyl-4-furoxancarbaldehydes



compd	R	radiochemical yield ^a (%)	radio purity ^a (%)	specific activity ^a (Ci/mmol)	dose ^b (mCi)	n ^c
[¹³ N] 1	methyl	34 ± 2	>99	0.3	23 ± 1	3
[¹³ N] 2	ethyl	14 ± 2	94 ± 3	0.5	11 ± 2	3
[¹³ N] 3	propyl	13 ± 6	94 ± 3	0.5	8 ± 4	3
[¹³ N] 4	isopropyl	11 ± 1	91 ± 2	1.3	8 ± 2	3
[¹¹ C] 5	methyl	21 ± 8	88 ± 3	220	25 ± 12	3

^aAssessed by HPLC after radiosynthesis and Sep Pak purification (decay corrected). ^bActivity in the dose (3 mL) after synthesis (typical synthesis time: ¹³N 20 min, ¹¹C, 60 min). ^cn is the number of repetitions.

NO-related bioactivities including: cytotoxicity,^{11,12} mutagenicity,¹³ central muscle relaxant,¹⁴ monamine oxidase inhibition,¹⁵ and blood pressure lowering activity.^{16–18} Pseudoaromatic properties help stabilize the ring against acids, electrophiles, and heat.^{19,20} However, they lack stability toward bases and nucleophiles.¹⁹ In furoxans, literature reports suggest that NO release occurs secondary to an attack by a thiolate at the 3- or 4-position leading to ring opening and elimination of nitrosyl anions.^{21–26}

Painful diabetic neuropathy (PDN) is a long-term complication of diabetes that is a type of peripheral neuropathic pain notoriously difficult to treat with clinically available analgesic and adjuvant drugs due to lack of efficacy and/or dose-limiting side-effects.²⁷ Recent work from the Smith laboratory has shown that the furoxan nitric oxide (NO) donor, PRG150 1 (3-methyl-4-furoxancarbaldehyde), produced potent dose-dependent pain relief in a rat model of PDN.^{27,28} However, information on the metabolic stability and biodistribution of PRG150 is lacking. Hence, the aims of the present study were to assess the *in vitro* metabolic stability of PRG150 using rat liver microsomes and to utilize PET-CT to assess the biodistribution of PRG150 following administration of single bolus intravenous (IV) and subcutaneous (SC) injection in adult male rats.

In nuclear medicine, positron emission tomography (PET) is a functional imaging technique that can be used to determine concentrations of radioactive tracers in the tissues of living organisms.²⁹ A tracer is composed of a biologically active molecule containing a short-lived radioactive isotope such as oxygen-15 (2 min), nitrogen-13 (10 min), carbon-11 (20 min), or fluorine-18 (110 min).³⁰ Using PET technology, biologic pathways can be traced to receptor sites of drug action. Combining a CT scan with a PET scan permits the images to be coregistered, which allows for accurate location of organs or other regions of interest (ROI). The mean activity in the ROI can be normalized using body weight and radioactivity injected to give standardized-uptake-values (SUV = ROI/(radioactivity injected × body weight)). The normalized data in the form of SUVs provides a more accurate comparison between separate imaging experiments. Furthermore, drug metabolites can be

easily located by their radioactivity. In general, radiolabeling and subsequent *in vivo* PET imaging provides a sophisticated noninvasive way to analyze drug action. However, the analysis of nitric oxide releasing furoxans, such as PRG150, presents a unique challenge because if NO release is to be monitored by PET imaging, nitrogen-13 must be used, despite its short half-life (10 min). When working with ¹³N, procedures and purification must be rapid to obtain an adequate dose.³¹ Fortunately, carbon metabolites can be imaged with longer-lived carbon-11 isotopes. Herein, we report a facile method for labeling and purifying ¹³N and ¹¹C labeled 3-methyl-4-furoxancarbaldehyde.

Fruttero et al. described the original synthesis of 3-methyl-4-furoxancarbaldehyde in 1989 and demonstrated by ¹H NMR spectroscopy that the aldehyde was quantitatively hydrated in water.³² The furoxan molecule was synthesized by reacting crotonaldehyde with nitrous acid. Due to the simplicity of this reaction, we thought a ¹³N-radiolabeled version could be feasible if ¹³NO₂⁻ could be produced. Unfortunately, there is no cyclotron target that produces solely ¹³NO₂⁻. Typically ¹³NH₄⁺ is produced by bombarding water containing ethanol as a reductant to quench oxidation.³¹ However, if the ethanol is omitted, radio yield favors ¹³NO₃⁻ with 1% ¹³NO₂⁻. Unfortunately, ¹³NO₃⁻ could not be used to make furoxans and so it must be reduced to ¹³NO₂⁻ prior to radiotracer synthesis.

Quantitative reduction of ¹³NO₃⁻ to ¹³NO₂⁻ can be achieved using a copperzinc cadmium reduction column.^{33–35} Once the crude cyclotron product is passed through a reduction column and subsequently a basic alumina Sep-Pak, ¹³NO₂⁻ is trapped on a small quaternary methylammonium (QMA) anion exchange cartridge. Concentrated saline (23.4% w/v; 0.15 mL) effectively eluted 90% of the radioactivity. With ¹³NO₂⁻ in hand, the furoxan was made by heating ¹³NO₂⁻ with crotonaldehyde, acetic acid, and sodium nitrite at 70 °C for 7 min. This method was also applied to other alkyl α,β-unsaturated aldehydes (Table 1).

In general, there was a decrease in radiochemical yield with increasing alkyl chain length, which is likely due to poor solubility under aqueous conditions. Attempts were made using preparative HPLC to purify ¹³N radiotracers, but a dose adequate for PET imaging could not be produced. Due to time constraints

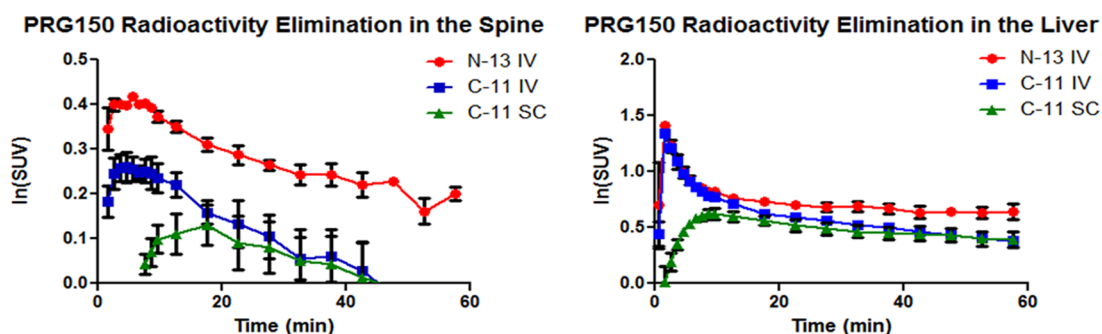


Figure 1. PET mean TACs (time-activity curves) of PRG150 in the spinal cord (left) and liver (right) ($n = 2$).

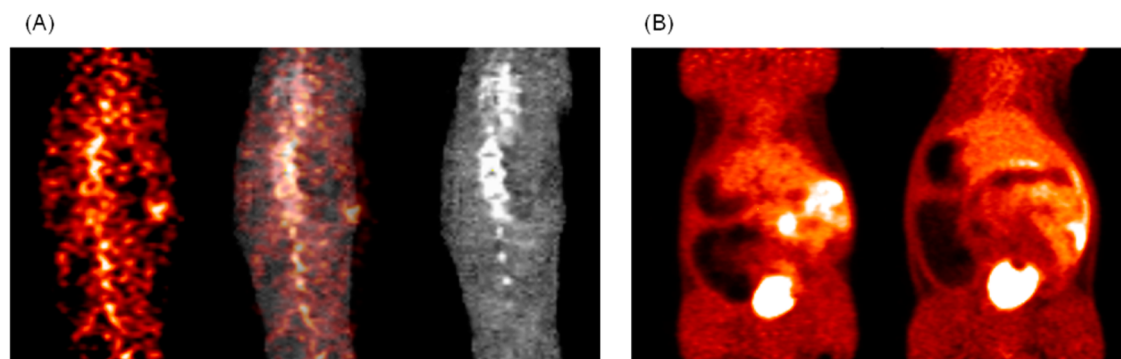


Figure 2. Rat PET images: (A) ^{13}N PRG150 in the spinal cord (left), coregistered (middle), and CT template (right). (B) Summed images 0–60 min post-tracer injection, ^{13}N PRG150 IV (left) and ^{11}C PRG150 IV (right).

when working with ^{13}N isotopes, purification was optimized experimentally by pressure transferring the crude reaction mixture through several Sep-Paks in series to produce a radiotracer of high radio and chemical purity (see Supporting Information).

After having optimized the purification procedure, it was hypothesized that a ^{11}C -labeling procedure could be designed and that the same Sep-Pak purification technique could be utilized, provided that similar conditions could be maintained. We envisioned making a ^{11}C -protected crotonaldehyde species 7 by using a Suzuki cross coupling reaction with pinacolboron precursor³⁶ 6 and ^{11}C methyl iodide followed by furoxan ring formation using nitrous acid (Table 1). The necessary ^{11}C intermediate was made by bubbling methyl iodide into a THF solution containing the precursor, palladium, ligand, and sodium acetate followed by heating for 10 min at 70 °C, which was adequate for the *in situ* conversion to ^{11}C diethoxy crotonaldehyde 7. After cooling, acetic acid was added, followed by sat. NaNO_2 . The reaction mixture was returned to the heating block for an additional 10 min. After cooling and diluting with water (deionized, 0.5 mL), the crude reaction mixture was pressure-transferred through the same Sep-Pak train used to purify the ^{13}N -derivative, using water (deionized, 3.25 mL) as eluent.

The synthesized ^{13}N and ^{11}C tracers were imaged in adult Sprague-Dawley rats ($n = 2$). Due to the short half-life of the radiotracers and unique molecule metabolism, it was essential for the animals to be anesthetized (isoflurane) and in the PET scanner prior to tracer administration. Tracers were injected intravenously through a tail vein catheter and dynamically imaged for 60 min. ^{13}N PRG150 time-SUV plots show major distribution in the cardiovascular system followed by the liver, kidneys, and bladder. ^{11}C PRG150 images also show major

uptake into the liver, kidneys, and bladder. In both cases, the ^{13}N and ^{11}C PRG150 radioactivity peaked in the liver at 1.5 min (Figure 1). In the kidneys, however, ^{13}N radioactivity peaked at 2.5 min, while the ^{11}C PRG150 peaked at 5.5 min. The discrepancy suggests that IV administered PRG150 is releasing NO almost immediately upon injection and that it is cleared quickly. The ^{11}C metabolite appears to remain in the systemic circulation until the kidneys filter it out shortly after the ^{13}N metabolites. A comparison of the radioactivity elimination in the spinal cord revealed a higher peak uptake of ^{13}N at 5.5 min, compared to ^{11}C in both IV (6.5 min) and SC (17.5 min) administration (Figures 1 and 2). In addition, ^{13}N radioactivity from PRG150 remained in the spinal cord outside of the 60 min PET scan window, while ^{11}C radioactivity was depleted after 45 min. The differences in radioactive uptake could indicate NO release at multiple levels of the somatosensory nervous system including the dorsal root ganglia and the spinal cord thereby contributing to the analgesic effects of PRG150 in the rat model of PDN^{8,37–39} by addressing the underlying depletion of NO bioactivity in this neuropathic pain condition.²⁶

The analgesic efficacy of PRG150 was assessed in the widely utilized streptozotocin-induced diabetic rat model of PDN following single bolus subcutaneous injection (SC) into the back of the neck. The time of onset of analgesia was 15 min, peak analgesia occurred after 60 min, and the duration of pain relief was ~ 3 h after single SC bolus dose administration.²⁷ To gain insight into the extended period of pain relief produced by single SC bolus doses of PRG150 in a rat model of PDN,²⁷ ^{11}C PRG150 was administered similarly, into the back of the neck of one adult male Sprague–Dawley rat. Using the radioactivity amount injected and animal weight to normalize PET-CT data to SUVs, the subcutaneous injection site ROI data was plotted and fitted with a biexponential trend line to estimate rates of distribution

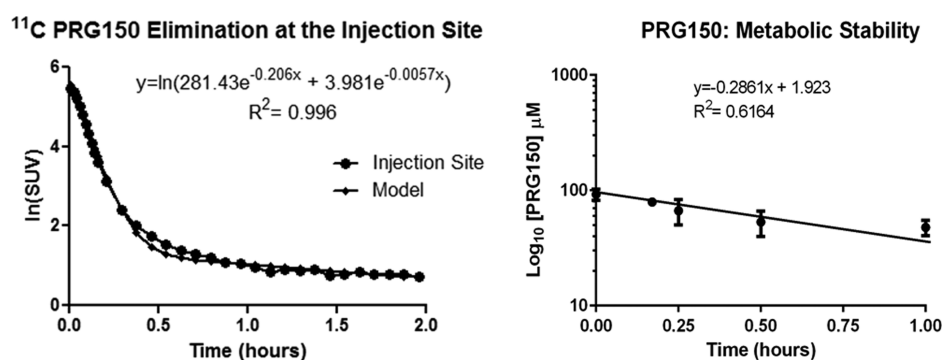


Figure 3. PET TAC (time-activity curve) of the subcutaneous injection site fitted with a biexponential model (left). The *in vitro* metabolic stability of PRG150 in rat liver microsomes (right).

and elimination with SC administration (Figure 3); the *in vivo* half-lives ($t_{1/2}$) of SC ^{11}C PRG150 were found to be 3 min in the distribution phase and 120 min in the elimination phase. The peak radioactive uptake in the spinal cord (17.5 min) correlates well to the onset of analgesia (15 min) seen in the rat model of PDN.²⁷ Also, there was a 37 min difference of peak radioactivity uptake in the kidneys when comparing IV (5.5 min) to SC administration (42.5 min) of ^{11}C PRG150. Slow elimination from the injection site and delayed kidney uptake could explain the longer duration of analgesia seen when PRG150 is administered subcutaneously.

For an *in vitro* comparison, the metabolic stability of PRG150 was assessed using rat liver microsomes. Specifically, rat liver microsomes (protein concentration, 1.2 mg/mL) were incubated with excess PRG150 (100 μM) at 37 °C in the presence of NADPH (1 mM). The percentage of PRG150 remaining in the microsomal incubates at each time of assessment was calculated by comparing the concentration of PRG150 remaining in the incubate at each sampling time, relative to the concentration at the start of incubation (0 min) that was arbitrarily assigned a value of 100%. It is important to note that in the control experiments ran in parallel, the concentration of PRG150 did not decrease when NADPH was omitted. The *in vitro* half-life ($t_{1/2}$) of PRG150 in rat liver microsomes was 2.4 h and the intrinsic clearance (CL_{int}) was 5.73 $\mu\text{L}/\text{min}\cdot\text{mg}$ protein (Figure 3). These *in vitro* parameter values are in the acceptable range for a novel compound with potential for human use as a novel analgesic to treat PDN.

In summary, to help elucidate the mechanism of analgesia seen in rat models of PDN with PRG150, methods were developed to label the furoxan moiety in two different positions to determine biodistribution in rats. Using $^{13}\text{NO}_2^-$, PRG150 and other 3-alkyl-furoxancarbaldehydes were labeled using nitrous acid to follow nitric oxide release with PET imaging. For a comparison, a method to synthesize ^{11}C PRG150 was developed to track the carbon metabolite. A Suzuki cross coupling of the boronate precursor **6** with ^{11}C methyl iodide furnished ^{11}C diethoxy crotonaldehyde **7** *in situ*. Using nitrous acid, ^{11}C PRG150 could be made in moderate radiochemical yield (^{13}N PRG150 34% and ^{11}C PRG150 21%) and good specific activity (^{13}N PRG150 0.3 Ci/mmol and ^{11}C PRG150 220 Ci/mmol). In addition, the ^{13}N and ^{11}C tracers could be purified quickly using only Sep-Paks and were subsequently administered to rats. Data from the PET-CT scans show an increase of ^{13}N radioactivity in the spinal cord compared to ^{11}C activity, indicating a possible site of action for the analgesic effects of PRG150. Both tracers behave similarly in the heart, liver, kidneys, and bladder. The *in vivo* and *in vitro* data

suggests PRG150 could potentially be a novel analgesic that could effectively treat painful diabetic neuropathy, a type of neuropathic pain that is difficult to treat.

■ ASSOCIATED CONTENT

📄 Supporting Information

The Supporting Information is available free of charge on the ACS Publications website at DOI: 10.1021/acsmedchemlett.5b00410.

Full experimental details are available for the synthesis of all compounds, radiosyntheses, HPLC purity tests, *in vitro* methods, animal studies, and PET images (PDF)

■ AUTHOR INFORMATION

Corresponding Author

*Tel: +1 404 712 1542. E-mail: apippin12@emory.edu.

Author Contributions

¹These authors contributed equally to this work and should be considered co-first authors.

Funding

This research was financially supported by a Queensland Emory Development (QED) grant from the National Center for Advancing Translational Sciences of the National Institutes of Health under Award Number UL1TR000454. The content is solely the responsibility of the authors and does not necessarily represent the official views of the National Institutes of Health. This research also utilized infrastructure purchased with funds from the Queensland Government's Smart State Research Facilities Fund as well as funds from the Australian Government's Super Science Translating Health Discovery Initiative from Therapeutic Innovation Australia (TIA) Ltd.

Notes

The authors declare the following competing financial interest(s): M.T.S. is named inventor on the PRG150 technology that has been licensed to QUE Oncology, a spin-off company formed by UQ and Emory University, for commercialization. M.T.S. undertakes contract R&D studies at UQ for multiple biopharmaceutical companies.

■ ACKNOWLEDGMENTS

We thank Ronald J. Crowe, Karen B. Dolph, and Michael S. Waldrep for assistance with radioisotope production and Margie Jones and Jaekeun Park for assistance with PET-CT animal imaging experiments.

■ ABBREVIATIONS

PDN, painful diabetic neuropathy; NO, nitric oxide; PRG150, 3-methyl-4-furoxancarbaldehyde; PET, positron emission tomography; μ PET, micropositron emission tomography; CT, computed tomography; Pd₂(dba)₃, tris(dibenzylideneacetone) dipalladium (0); ROI, region of interest; SC, subcutaneous; IV, intravenous; SUV, standard uptake value; QMA, quaternary methylammonium; NADPH, nicotinamide adenine dinucleotide phosphate

■ REFERENCES

- (1) Esplugues, J. V. NO as a Signaling Molecule in the Nervous System. *Br. J. Pharmacol.* **2002**, *135*, 1079–1095.
- (2) Hou, Y. C.; Janczuk, A.; Wang, P. G. Current Trends in the Development of Nitric Oxide Donors. *Curr. Pharm. Des.* **1999**, *5*, 417–441.
- (3) Thomas, D. D.; Liu, X.; Kantrow, S. P.; Lancaster, J. R. The Biological Lifetime of Nitric Oxide: Implications for the Perivascular Dynamics of NO and O₂. *Proc. Natl. Acad. Sci. U. S. A.* **2001**, *98*, 355–360.
- (4) Ischiropoulos, H. Biological Tyrosine Nitration: A Pathophysiological Function of Nitric Oxide and Reactive Oxygen Species. *Arch. Biochem. Biophys.* **1998**, *356*, 1–11.
- (5) Gödecke, A.; Schrader, J.; Reinartz, M. Nitric Oxide-Mediated Protein Modification in Cardiovascular Physiology and Pathology. *Proteomics: Clin. Appl.* **2008**, *2*, 811–822.
- (6) Jin, R. C.; Loscalzo, J. Vascular Nitric Oxide: Formation and Function. *J. Blood Med.* **2010**, 147–162.
- (7) Stamler, J. S.; Meissner, G. Physiology of Nitric Oxide in Skeletal Muscle. *Physiol. Rev.* **2001**, *81*, 209–237.
- (8) Cury, Y.; Picolo, G.; Gutierrez, V. P.; Ferreira, S. H. Pain and Analgesia: The Dual Effect of Nitric Oxide in the Nociceptive System. *Nitric Oxide* **2011**, *25*, 243–254.
- (9) Hirst, D.; Robson, T. Targeting Nitric Oxide for Cancer Therapy. *J. Pharm. Pharmacol.* **2007**, *59*, 3–13.
- (10) Wallace, J. L. Nitric Oxide as a Regulator of Inflammatory Processes. *Mem. Inst. Oswaldo Cruz.* **2005**, *100*, 5–9.
- (11) Boiani, M.; Cerecetto, H.; González, M.; Risso, M.; Olea-Azar, C.; Piro, O. E.; Castellano, E. E.; López de Ceráin, A.; Ezpeleta, O.; Monge-Vega, A. 1,2,5-Oxadiazole N-Oxide Derivatives as Potential Anti-Cancer Agents: Synthesis and Biological Evaluation. Part IV. *Eur. J. Med. Chem.* **2001**, *36*, 771–782.
- (12) Cerecetto, H.; González, M. Benzofuroxan and Furoxan. Chemistry and Biology. *Top. Heterocycl. Chem.* **2007**, *10*, 265–308.
- (13) Balbo, S.; Lazzarato, L.; Di Stilo, A.; Fruttero, R.; Lombaert, N.; Kirsch-Volders, M. Studies of the Potential Genotoxic Effects of Furoxans: the Case of CAS 1609 and of the Water-Soluble Analogue of CHF 2363. *Toxicol. Lett.* **2008**, *178*, 44–51.
- (14) Bertinaria, M.; Stilo, A. D.; Tosco, P.; Sorba, G.; Poli, E.; Pozzoli, C.; Coruzzi, G.; Fruttero, R.; Gasco, A. [3-(1H-Imidazol-4-Yl)Propyl]-Guanidines Containing Furoxan Moieties. *Bioorg. Med. Chem.* **2003**, *11*, 1197–1205.
- (15) Severina, I. S.; Axenova, L. N.; Veselovsky, A. V.; Pyatakova, N. V.; Buneeva, O. A.; Ivanov, A. S.; Medvedev, A. E. Nonselective Inhibition of Monoamine Oxidases A and B by Activators of Soluble Guanylate Cyclase. *Biochemistry (Moscow)* **2003**, *68*, 1048–1054.
- (16) Gasco, A.; Fruttero, R.; Sorba, G.; Di Stilo, A.; Calvino, R. NO Donors: Focus on Furoxan Derivatives. *Pure Appl. Chem.* **2004**, *76*, 973–981.
- (17) Aguirre, G.; Boiani, M.; Cerecetto, H.; Fernández, M.; González, M.; León, E.; Pintos, C.; Raymondo, S.; Arredondo, C.; Pacheco, J. P. Furoxan Derivatives as Cytotoxic Agents: Preliminary *in vivo* Antitumoral Activity Studies. *Pharmazie* **2006**, *61*, 54–59.
- (18) Bohn, H.; Brendel, J.; Martorana, P. A.; Schönafinger, K.; Lombaert, N. Cardiovascular Action of the Furoxan CAS 1609, A Novel Nitric Oxide Donor. *Br. J. Pharmacol.* **1995**, *114*, 1605–1612.
- (19) Wang, P. A.; Xian, M.; Tang, X.; Wu, X.; Wen, Z.; Cai, T.; Janczuk, A. J. Nitric Oxide Donors: Chemical Activities and Biological Applications. *Chem. Rev.* **2002**, *102*, 1091–1134.
- (20) Pasinszki, T.; Havasi, B.; Hajgató, B.; Westwood, N. P. C. Synthesis, Spectroscopy and Structure of the Parent Furoxan (HCNO) 2. *J. Phys. Chem. A* **2009**, *113*, 170–176.
- (21) Medana, C.; Ermondi, G.; Fruttero, R. Furoxans as Nitric Oxide Donors. 4-Phenyl-3-Furoxanarbonitrile: Thiol-Mediated Nitric Oxide Release and Biological Evaluation. *J. Med. Chem.* **1994**, *37*, 4412–4416.
- (22) Ferioli, R.; Folco, G. C.; Ferretti, C.; Gasco, A. M.; Medana, C.; Fruttero, R.; Civelli, M.; Gasco, A. A New Class of Furoxan Derivatives as NO Donors: Mechanism of Action and Biological Activity. *Br. J. Pharmacol.* **1995**, *114*, 816–820.
- (23) Di Stilo, A.; Cena, C.; Gasco, A. M.; Gasco, A.; Ghigo, D. Glutathione Potentiates cGNP Synthesis Induced by the Two Phenylfuroxanarbonitrile Isomers in RFL-6 Cells. *Bioorg. Med. Chem. Lett.* **1996**, *6*, 2607–2612.
- (24) Sako, M.; Oda, S.; Ohara, S.; Hirota, K.; Maki, Y. Facile Synthesis and NO-Generating Property of 4H-[1,2,5]Oxadiazolo[3,4-D]-Pyrimidine-5,7-Dione 1-Oxides. *J. Org. Chem.* **1998**, *63*, 6947–6951.
- (25) Nirole, W. F.; Luis, J. M.; Wicker, J. F.; Wachter, N. M. Synthesis and Evaluation of NO-Release From Symmetrically Substituted Furoxans. *Bioorg. Med. Chem. Lett.* **2006**, *16*, 2299–2301.
- (26) Sorba, G.; Medana, C.; Fruttero, R.; Cena, C.; Di Stilo, A.; Galli, U.; Gasco, A. Water Soluble Furoxan Derivatives as NO Prodrugs. *J. Med. Chem.* **1997**, *40*, 463–469.
- (27) Huang, L. Y.; Tsui, D. Y.; Williams, C. M.; Wyse, B. D.; Smith, M. T. The Furoxan Nitric Oxide Donor, PRG150, Evokes Dose-Dependent Analgesia in a Rat Model of Painful Diabetic Neuropathy. *Clin. Exp. Pharmacol. Physiol.* **2015**, *42*, 921–929.
- (28) Smith, M. T. Pain-Relieving Compositions and Uses Therefor. Google Patents US 2015/0051404 A1, 2015.
- (29) Ametamey, S. M.; Honer, M.; Schubiger, P. A. Molecular Imaging with PET. *Chem. Rev.* **2008**, *108*, 1501–1516.
- (30) Miller, P. W.; Long, N. J.; Vilar, R.; Gee, A. D. Synthesis of ¹¹C, ¹⁸F, ¹⁵O, and ¹³N Radiolabels for Positron Emission Tomography. *Angew. Chem., Int. Ed.* **2008**, *47*, 8998–9033.
- (31) Gómez-Vallejo, V.; Gaja, V.; Gona, K. B.; Llop, J. Nitrogen-13: Historical Review and Future Perspectives. *J. Labelled Compd. Radiopharm.* **2014**, *57*, 244–254.
- (32) Fruttero, R.; Ferrarotti, B.; Serafino, A.; Di Stilo, A.; Gasco, A. Unsymmetrically Substituted Furoxans. Part 11. Methylfuroxancarbaldehydes. *J. Heterocycl. Chem.* **1989**, *26*, 1345–1347.
- (33) Thabano, J. R. E.; Abong'o, D.; Sawula, G. M. Determination of Nitrate by Suppressed Ion Chromatography After Copperised-Cadmium Column Reduction. *J. Chromatogr. A* **2004**, *1045*, 153–159.
- (34) Llop, J.; Gómez-Vallejo, V.; Bosque, M.; Quincoces, G.; Peñuelas, I. Synthesis of S-[¹³N]nitrosogluthathione (¹³N-GSNO) as a New Potential PET Imaging Agent. *Appl. Radiat. Isot.* **2009**, *67*, 95–99.
- (35) Gómez-Vallejo, V.; Kato, K.; Oliden, I.; Calvo, J.; Baz, Z.; Borrell, J. I.; Llop, J. Fully Automated Synthesis of ¹³N-Labeled Nitrosothiols. *Tetrahedron Lett.* **2010**, *51*, 2990–2993.
- (36) Touré, B. B.; Hoveyda, H. R.; Taylor, J.; Ulaczyk-Lesanko, A.; Hall, D. G. A Three-component Reaction for Diversity-Oriented Synthesis of Polysubstituted Piperidines: Solution and Solid-Phase Optimization of the First Tandem Aza[4 + 2]/Allylboration. *Chem. - Eur. J.* **2003**, *9*, 466–474.
- (37) Schaible, H. *Pain Control*; Springer, 2015.
- (38) Tsukahara, H.; Kaneko, K. *Studies on Pediatric Disorders*; Springer, 2014.
- (39) Mahmoud, M. A.; Fahmy, G. H.; Moftah, M. Z.; Sabry, I. Distribution of Nitric Oxide-Producing Cells Along Spinal Cord in Urodeles. *Front. Cell. Neurosci.* **2014**, *8*, 1–7.